中國機械工程學刊第四十一卷第二期第 169~179 頁(民國一百零九年)
Journal of the Chinese Society of Mechanical Engineers, Vol.41, No.2, pp 169~179 (2020)

Subdivision Control Algorithm Based on Fuzzy-PID Decoupling for Ship Dynamic Positioning

Hong-sheng Li*, Meng Wang**, Thierno-Mamadou-Pathe Diallo*** and Qing Miao**

Keywords: Dynamic Positioning, Subdivision Control, Decoupling Control, Fuzzy-PID

ABSTRACT

Dynamic positioning is to keep ship at a set position in the sea by its own power, which is a complex process because of complexity of ship motion and uncertainness of marine environment. In this paper, subdivision control algorithm based on fuzzy-PID is developed, and is used for keeping ship's position under the effect of external load. On the inner loop, decoupling control method based on motion model of three degree of freedom (3-DOF) is adopted to remove the coupling between controlled variables. Fuzzy-PID dual mode controller is designed to control the velocity and angular velocity. Fuzzy switching logic (FSL) is adopted to decrease the switching disturbance of Fuzzy-PID dual mode controller. On the outer loop, subdivision control strategy is used to control the position and heading. This method constitutes the cascade control system and is used to realize the accurate positioning. The simulations and experiments are conducted by using this control method to verify its high positioning accuracy, strong adaptability to environment and certain robustness.

INTRODUCTION

Dynamic positioning system (DPS) is to keep ship at a predetermined position or predetermined track for marine operation purposes by its own power without the help of a mooring system. DPS is generally consisted of position measurement system, control system and thruster system. The basic functions are fixed point control and track control. In fixed point control mode, ship can automatically move to its set position after its real position diverges from the set value. In track control mode, DPS can navigate ship along a predetermined trajectory.

DPS has been applied to ship since the 1960s, and today it is equipped on many new ships used for freight transport, offshore exploration and exploitation (Bui *et al.*, 2012). Many control techniques are used in DPS (Fossen and Perez, 2009; Zhang *et at.*, 2013; John *et al.*, 1982; Akasaka, 2006; Wang *et al.*, 2013; Tee and Sam, 2006). In the 1960s, PID controllers were applied to controlling the horizontal motion of ships (surge, sway and yaw) by means of thrusters and propellers. This product adopts the conventional PID control technology. Subsequently, control technology based on the modern control theory is applied to DPS. That is known as the second generation of DPS. Since then, Nonlinear PID-control, passive observer design and observer backstepping are designed for DPS (Fossen and Grovlen, 1998; Grorvlen and Fossen, 1996). The third generation of DPS is based on intelligent control theory and method, for example the robust control, fuzzy control (Boulkroune *et al.*, 2014; Chen and Tan, 2011), nonlinear model predictive control etc. Due to more stable and accurate measuring equipment and more advanced control method applied, DPS has high accuracy, strong adaptability, strong robustness and intelligence (McGookin *et al.*, 2000; Ding and Mao, 1998).

Hybrid control has been applied to DPS these years. Hybrid control can realize the switching between multiple controllers according to different environment. The designed system will automatically switch to corresponding filtering algorithm and control algorithm in certain sea conditions. By this, DPS can expand the ship's working range and anti-interference ability (Dong *et al.*, 2006). Hybrid of fuzzy and PID control algorithm is proposed in the references (Liu *et al.*, 2002; Parnichkun and

Paper Received November 2017. Revised April, 2018. Accepted May, 2018. Author for Correspondence: Meng Wang.

** Professor, School Of Mechanical and Electronic Engineering, Wuhan University of Technology, Wuhan, China.*

*** Ph.D. student, School Of Mechanical and Electronic Engineering, Wuhan University of Technology, Wuhan, China.*

**** Professor, Faculty of Science, Centre Universitaire de Kindia, Kindia.*

Ngaecharoenkul, 2001). This control algorithm is separated into two parts: fuzzy control and PID control. This kind controller has both advantages of fuzzy control and PID control. It has better rapidity and less dynamical error than fuzzy control, and has stronger robustness than PID control. Fuzzy switching controller based on supervision has been put forward and applied to DPS. Conventional PID controller and fuzzy controller are combined together by a fuzzy switching mode (Wang and Jia, 2006). Supervisory level controls the switching between two controllers according to the input of trajectory deviation. This control method can not only take full advantages of different control methods, but effectively avoid the phenomenon of non-smooth switching process (Jia *et al.*, 2005).

This paper takes a 3.75m test ship as the research object. The main objective is to find a control law to keep the position and heading of the ship at a set value, and be able to maintain high control precision under certain marine environment. Ship mathematical model is presented in Section 2. Control methods of outer loop and inner loop are detailed in Section 3 and Section 4. The simulations are conducted by using simulation software MATLAB in Section 5. Experiments are carried out in the PC experimental platform in Section 6. Finally, conclusions are presented in Section 7.

SHIP MOTION MATHEMATICAL MODEL

In order to describe ship movement, two kinds of coordinate system are usually adopted, namely fix coordinate system and body coordinate system as indicated in Figure 1.

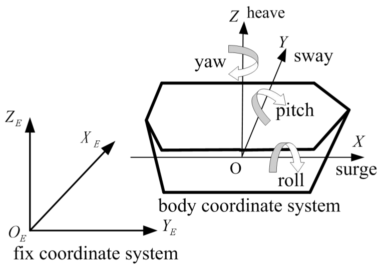

Fig. 1. Two kinds of coordinate reference system

Fix coordinate system $O_E - X_E Y_E Z_E$ can be considered to be inertial. The position and heading of ship should be described relative to the inertial reference frame. Fix coordinate system in hydrostatic plane is fixed at any point of the earth's surface. Body coordinate system is not an inertial frame of reference, and it has velocity and angular velocity relative to the ground. When analyzing ship motion, we should transfer the first established equation in fix coordinate system to body coordinate system and get corresponding motion equations.

The reduced motion equations of DPS in surge, sway, and yaw can be expressed as follows (Verma, 2004; Chang *et al.*, 2002; Kim, 2000):

$$\begin{cases} M\upsilon' + D\upsilon = \tau \\ \eta' = J(\psi)\upsilon \end{cases}, \tag{1}$$

where $\upsilon = [u,v,r]^T \in R^3$ denotes the low-frequency velocity vector, τ is a vector of control forces and torque, $\eta = [x,y,\psi]^T$ denotes the position and heading vector in fix coordinate system, $J(\psi)$ is a velocity transformation matrix that transforms velocities of body coordinate system to fix coordinate system. $J(\psi)$ is given by:

$$J(\psi) = \begin{bmatrix} \cos(\psi) & -\sin(\psi) & 0 \\ \sin(\psi) & \cos(\psi) & 0 \\ 0 & 0 & 1 \end{bmatrix}. \tag{2}$$

The inertia matrix M is assumed to be positive definite, and $D > 0$ is a matrix representing linear hydrodynamic damping (Liu, 2010).

In this paper, the control object is the test ship. By the numerical method, inertia matrix and damping matrix is obtained. They are as follows:

$$M = \begin{bmatrix} 0.754 & 0 & 0 \\ 0 & 1.199 & 0.211 \\ 0 & 0.029 & 0.524 \end{bmatrix}, \tag{3}$$

$$D = \begin{bmatrix} 0.014 & 0 & 0 \\ 0 & 0.102 & -0.024 \\ 0 & 0.192 & 0.095 \end{bmatrix}. \tag{4}$$

SUBDIVISION CONTROL FOR THE OUTER POSITION LOOP

The frame of DPS cascade control system is shown in Figure 2. The output of subdivision controller is the set value of velocity and angle velocity, and is also the input of inner loop.

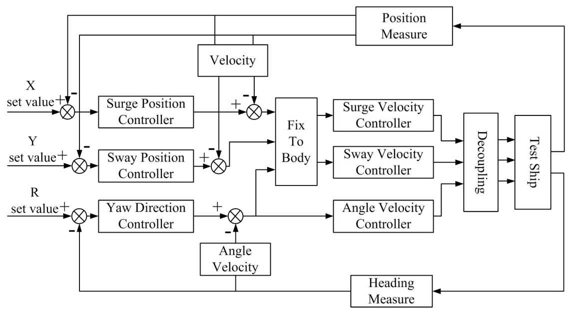

Fig. 2. Control structure of DPS

Subdivide Mode of Subdivision Control

This paper adopts subdivision control strategy for the outer loop. Deviation signals are divided into several levels, and different velocity is set at different levels. When the deviation is at a high level, we set higher velocity. So the ship is in rapid motion mode. When deviation becomes small, we set lower velocity. The ship is in slow motion mode.

The error is divided into large level ($e > e_B$), moderate level ($e_B > e > e_M$) and small level ($e < e_B$). e is the error on a certain DOF. e_B and e_M are scale value. Subdivision mode is shown in Figure 3.

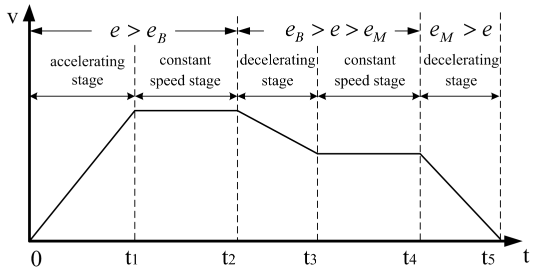

Fig. 3. Subdivision mode

The Setting of Velocity Curve

Velocity setting for different mode should consider the motion characteristic of DP ship and physical limit for thruster system. If set value of velocity is too large, it leads overshoot. If the setting is too small, the control process is slow, and settling time becomes long. Taking surge loop for example and according to above conditions, we design set velocity values as fallowing:

Rapid motion mode (error range: $e > 1.5m$)

Accelerating stage: $v_{set} = (0.01 + v_0)\ m/s$

Constant speed stage: $v_{set} = 0.1\ m/s$

Slow motion mode (error range: $1.5m > e > 0.5m$)

Decelerating stage: $v_{set} = (v_0 - 0.01)\ m/s$

Constant speed stage: $v_{set} = 0.02\ m/s$

Approach mode (error range: $e < 0.5m$)

Decelerating stage: $v_{set} = (0.04 \cdot e)\ m/s$.

By this way, it can not only divide process of movement into several modes and stages clearly, but also avoids large amount of instantaneous controlled quantity during switching between two stages.

FUZZY-PID DECOUPLING CONTROL FOR THE INNER VELOCITY LOOP

The role of vice loop is to make velocity of surge and sway and angle velocity of yaw follow output of the main circuit rapidly. The vice controller utilizes fuzzy-PID dual mode control. The block diagram is shown in Figure 4.

Set values in inner loop are given by subdivision controller in out loop and have been transformed from fix coordinate system to body coordinate system. Fuzzy-PID dual-mode control based on fuzzy switch logic is applied to realize switching without disturbance and achieve dynamic and steady state performance. Decoupling control is designed to remove the decoupling between sway loop and yaw loop.

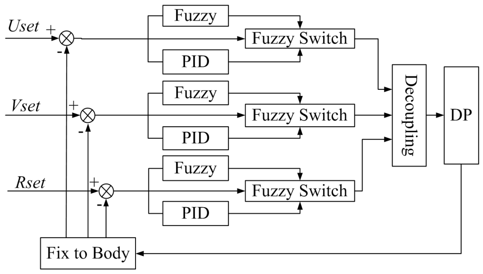

Fig. 4. Block diagram of inner loop

Decoupling Control

Aiming at DP ship, this paper adopts feed-forward compensation decoupling method. Feed-forward compensation decoupling makes the decoupling device in forward channel. According to the motion model of 3-DOF, we establish decoupling structures of sway loop and yaw loop. Figure 5 is the block diagram of feed-forward compensation decoupling. As we add decoupling compensation in feed forward channel, the coupling is eliminated by feed-forward.

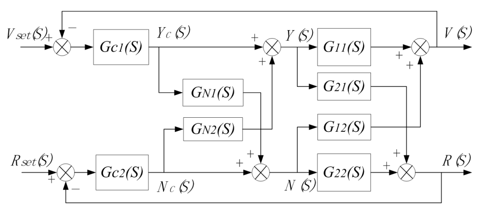

Fig. 5. Feed-forward compensation decoupling

$V_{set}(S)$ and $R_{set}(S)$ are the set velocity of sway loop and angle velocity of yaw loop. $V(S)$ and $R(S)$ are the velocity and angle velocity output of the ship. $G_{11}(S)$, $G_{12}(S)$, $G_{21}(S)$ and $G_{22}(S)$ consist a coupling relationship of controlled ship. $G_{N1}(S)$ and $G_{N2}(S)$ are feed-forward compensation taches that will be designed. $G_{C1}(S)$ and $G_{C2}(S)$ are the controllers of sway loop and yaw loop. $Y_C(S)$ and $N_C(S)$ are outputs of controllers. Correspondingly, $Y(S)$ and $N(S)$ are actual control force and control torque. The purpose is to realize decoupling between $Y_C(S)$ and $R(S)$, decoupling between $N_C(S)$ and $V(S)$. Based on the Fig. 5, we can get the following equations:

$$\begin{bmatrix} V(S) \\ R(S) \end{bmatrix} = \begin{bmatrix} G_{11}(S) & G_{12}(S) \\ G_{21}(S) & G_{22}(S) \end{bmatrix} \begin{bmatrix} Y(S) \\ N(S) \end{bmatrix}, \tag{5}$$

$$\begin{bmatrix} Y(S) \\ N(S) \end{bmatrix} = \begin{bmatrix} 1 & G_{N2}(S) \\ G_{N1}(S) & 1 \end{bmatrix} \begin{bmatrix} Y_C(S) \\ N_C(S) \end{bmatrix}. \tag{6}$$

According to equation (5) and equation (6), we have:

$$\begin{aligned} \begin{bmatrix} V(S) \\ R(S) \end{bmatrix} &= \begin{bmatrix} G_{11}(S) & G_{12}(S) \\ G_{21}(S) & G_{22}(S) \end{bmatrix} \begin{bmatrix} 1 & G_{N2}(S) \\ G_{N1}(S) & 1 \end{bmatrix} \begin{bmatrix} Y_C(S) \\ N_C(S) \end{bmatrix} \\ &= \begin{bmatrix} G_{11}(S)+G_{12}(S)G_{N1}(S) & G_{11}(S)G_{N2}(S)+G_{12}(S) \\ G_{21}(S)+G_{22}(S)G_{N1}(S) & G_{21}(S)G_{N2}(S)+G_{22}(S) \end{bmatrix} \begin{bmatrix} Y_C(S) \\ N_C(S) \end{bmatrix}. \end{aligned} \tag{7}$$

Based on feed-forward compensation decoupling theory, the transfer functions of compensation taches are:

$$\begin{cases} G_{N1}(S) = -G_{22}^{-1}(S)G_{21}(S) \\ G_{N2}(S) = -G_{11}^{-1}(S)G_{12}(S) \end{cases}, \tag{8}$$

where $G_{11}(S)$ and $G_{22}(S)$ are different to zero. Then we can arrive at:

$$\begin{bmatrix} V(S) \\ R(S) \end{bmatrix} = \begin{bmatrix} G_{11}(s)+G_{12}(s)G_{N1}(s) & 0 \\ 0 & G_{21}(s)G_{N2}(s)+G_{22}(s) \end{bmatrix} \begin{bmatrix} Y_C(S) \\ N_C(S) \end{bmatrix}. \tag{9}$$

According to the motion model of 3-DOF, coupling exist in movement of sway and yaw. The differential equations for the two directions are as follows:

$$1.199v'(t) + 0.211r'(t) + 0.102v(t) - 0.024r(t) = y(t), \tag{10}$$

$$0.029v'(t) + 0.524r'(t) + 0.192v(t) - 0.095r(t) = n(t). \tag{11}$$

Assuming that the initial velocity is equal to zero, the Laplace transforms of $y(t)$ and $n(t)$ are given by the following system:

$$\begin{bmatrix} 1.199S+0.102 & 0.211S-0.024 \\ 0.029S+0.192 & 0.524S+0.095 \end{bmatrix} \begin{bmatrix} V(S) \\ R(S) \end{bmatrix} = \begin{bmatrix} Y(S) \\ N(S) \end{bmatrix}, \tag{12}$$

where we can get:

$$\begin{bmatrix} V(S) \\ R(S) \end{bmatrix} = \begin{bmatrix} G_{11}(S) & G_{12}(S) \\ G_{21}(S) & G_{22}(S) \end{bmatrix} \begin{bmatrix} Y(S) \\ N(S) \end{bmatrix}, \tag{13}$$

$$G_{11}(S) = \frac{0.524S+0.095}{0.6222S^2+0.1275S+0.0143}, \tag{14}$$

$$G_{11}(S) = -\frac{0.211S-0.024}{0.6222S^2+0.1275S+0.0143}, \tag{15}$$

$$G_{11}(S) = -\frac{0.029S+0.192}{0.6222S^2+0.1275S+0.0143}, \tag{16}$$

$$G_{11}(S) = \frac{1.199S+0.102}{0.6222S^2+0.1275S+0.0143}. \tag{17}$$

Based on the above analysis, we can determine the coupling structure of the test ship. All parts' transfer functions in Fig. 5 are given by $G_{11}(S)$, $G_{12}(S)$, $G_{21}(S)$ and $G_{22}(S)$.

The transfer functions of feed-forward decoupling compensation taches are given by

$$G_{N1}(S) = \frac{0.029S+0.192}{1.199S+0.102}, \quad G_{N1}(S) = \frac{0.211S+0.024}{0.524S+0.095}. \tag{18}$$

After decoupling, relations between controller outputs ($Y_C(S)$ and $N_C(S)$) and system outputs ($R(S)$ and $V(S)$) are:

$$Y_C(S)G_{11}(S) + Y_C(S)G_{N1}(S)G_{12}(S) = V(S), \tag{19}$$

$$N_C(S)G_{22}(S) + N_C(S)G_{N2}(S)G_{21}(S) = R(S). \tag{20}$$

So, the transfer functions of sway direction and yaw direction are:

$$\frac{V(S)}{Y_C(S)} = \frac{1}{1.199S+0.102}, \quad \frac{R(S)}{N_C(S)} = \frac{1}{0.524S+0.095}. \tag{21}$$

Fuzzy-PID Dual Mode Control based on Fuzzy Switching Rules

In last section, the transfer functions of sway loop and yaw loop are calculated respectively. According to the structure, it is first order system between force and displacement, and the parameters of PID control are obtain according trial and error method as:

$$P_{surge} = 0.5, I_{surge} = 0.04, D_{surge} = 0.4, \tag{22}$$

$$P_{sway} = 0.6, I_{sway} = 0.06, D_{sway} = 0.6, \tag{23}$$

$$P_{yaw} = 0.3, I_{yaw} = 0.05, D_{yaw} = 0.2. \tag{24}$$

Then, the closed-loop transfer functions of three loops are obtained as:

$$\Phi_{surge}(S) = \frac{U(s)}{U_{set}(S)} = \frac{S}{1.154S^2+0.514S+0.04}, \tag{25}$$

$$\Phi_{sway}(S) = \frac{V(s)}{V_{set}(S)} = \frac{S}{1.799S^2+0.702S+0.06}, \tag{26}$$

$$\Phi_{yaw}(S) = \frac{R(s)}{R_{set}(S)} = \frac{S}{0.724S^2+0.395S+0.05}. \tag{27}$$

Figures 6-8 show the performance of velocity response for three loops by using the selected PID parameters. The result shows the PID controller has fast response and small overshoot.

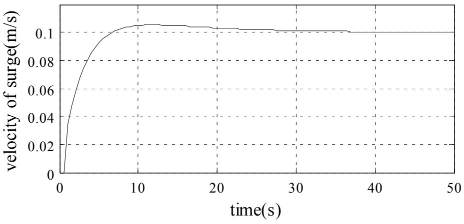

Fig. 6 Velocity response of surge

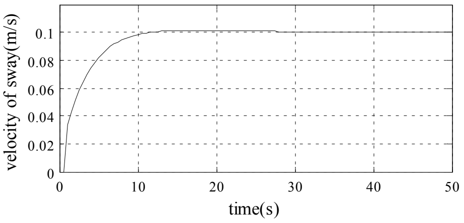

Fig. 7 Velocity response of sway

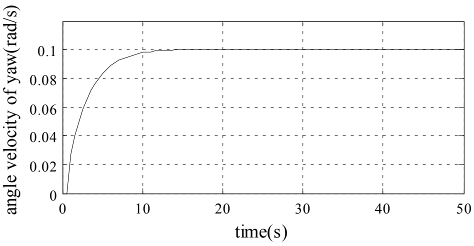

Fig. 8 Velocity response of yaw

PID controllers have simple control structures, high stable precision and effectiveness for linear systems (Chen, 1996; Li, 1998; Bandyopadhyay and Patranabis, 2001; Dey and Mudi, 2009; Kim and Oh, 2000). In fact, the important parameters *M* and *D* in equation (1) is mainly obtained through numerical methods, which cannot ensure the accuracy of parameters. Considering that FLS has good robustness and makes it possible to overcome the adverse effects of uncertain factors brought to the system, such as variations and nonlinear model, a kind of hybrid of fuzzy and PID control is adopt for the control of DP. Conventional PID controller and a fuzzy logic controller (FLC) are combined in order to obtain the advantages of both PID and FLC. This is useful to ensure fast response and good stable accuracy of the system.

When the velocity deviation is large, switching logic will switch to the fuzzy controller. When the velocity deviation is small, switching logic will switch to the PID controller in order to obtain a better steady-state performance. In this way, the speed loop will get a better control effect with dynamic and steady state performance.

Taking surge loop as example, velocity deviation e_{body} and change of deviation ec_{body} are inputs of the controller, where $e_{body} = u_{set} - u$ and $ec_{body} = de_{body} / dt$. u_{set} and u are the set velocity and real velocity in surge direction. The steps for designing the proposed controller for DPS are summarized as follows:

(1) Once the fuzzy controller inputs and outputs are chosen, we define the universe of discourse for the input and output variables. We use the error signal and change of error signal. Fuzzy domain of input variables E and EC is $[-6,6]$ while fuzzy domain of output of variable is $[-6,6]$. Actual domains of deviation, change of deviation and control quantity are $[-0.02,0.02]$, $[-0.02,0.02]$, $[-0.015,0.015]$. So here are the determined quantization factors of deviation, the change of deviation, and the control quantity: $k_e = 300$, $k_{ec} = 300$ and $k_u = 0.0025$.

(2) For convenience, membership functions (MFs) of inputs and output are chosen as triangle-shaped MF. Figures 9-10 show the MFs for the error signal, change of error signal, and output respectively, where the universe of discourse is divided into seven overlapping linguistic: labeled positive large (PL), positive middle (PM), positive small (PS), zero (ZR), negative small (NS), negative middle (NM), and negative large (NL).

(3) According to practical experiences, 49 fuzzy IF-THEN rules are designed as fuzzy logic. The fuzzy control rules are expressed in table 1 correspondingly.

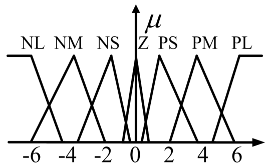

Fig. 9. MFs of inputs

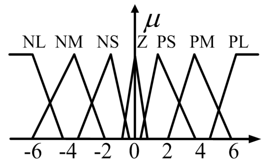

Fig. 10. MFs of output

Table 1 Rule base

EC	***DU***						
	E						
	NL	**NM**	**NS**	**Z**	**PS**	**PM**	**PL**
NL	NL	NL	NL	NM	NS	PS	PM
NM	NL	NL	NM	NM	Z	PS	PM
NS	NL	NL	NS	NS	Z	PM	PM
Z	NL	NM	NS	Z	PS	PM	PL
PS	NM	NM	Z	PS	PS	PL	PL
PM	NM	NS	Z	PM	PM	PL	PL
PL	NM	NS	PS	PM	PL	PL	PL

(4) When the fuzzy output is calculated, it must be transformed into a numeric value which can be recognized by thruster allocation algorism in DPS. There are several methods to achieve this transformation. In this work, the method of

center-average defuzzifier previously introduced is applied. Center-average is the most reasonable defuzzification method whose physical significance express the center of area enclosed by membership function curve and the horizontal axis. It also contains all the information of fuzzy output, thus it's more reasonable.

In this paper, FLS is used to satisfied fast response while PID control is used to reduced error to a minimum. Fuzzy controller and PID controller are combined based on fuzzy switching rules, which uses deviation of velocity as feature variable to make decision. Taking surge loop as example, the dual mode controller can switch between fuzzy and PID according to the following rules: If e is Z and ec is Z, then u is u_{PID} , Else u is u_{Fuzzy} . u_{Fuzzy} and u_{PID} are outputs of fuzzy controller and PID controller. MFs of fuzzy switching rules are shown in Figures 11-12.

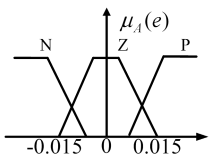

Fig. 11. MFs of e

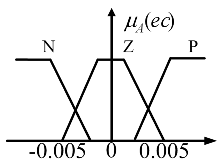

Fig. 12. MFs of ec

By the MFs we can obtain the weight values of output of controllers at each sampled time such as:

$$\omega_{PID} = \theta^T \psi(x) = \frac{\sum_{i=1}^{9} f^i (\prod_{j=1}^{2} \mu_{A_j^i}(x_j))}{\sum_{i=1}^{9} (\prod_{j=1}^{2} \mu_{A_j^i}(x_j))}, \tag{28}$$

$$\omega_{Fuzzy} = 1 - \omega_{PID} . \tag{29}$$

So the output of fuzzy-PID dual mode controller can be written as $u = \omega_{PID} u_{PID} + \omega_{Fuzzy} u_{Fuzzy}$.

SIMULATION

The simulations are carried out using ship model. The purpose of the simulations is to verify the feasibility of the designed control algorithm. By using MATLAB/SIMULINK, we have established the simulation model. Initial inputs are $[x, y, \psi]^T$ in fix coordinate system. The force from wind, wave and flow, as disturbance, acts to the ship. According to the parameters of test ship model, we select 0.5s as simulation sampling time. Surge power and sway power are limited to $0.05kN$. Torque is limited to $0.05kN \cdot m$. Control cycle is $0.5s$. Time lag is $0.5s$.

In Calm Water

In calm water condition, the external load is zero. Initial inputs are set as $[x, y, \psi]^T = [5m, 5m, 0.3rad]$. Figures 13-16 show the simulation results in calm water.

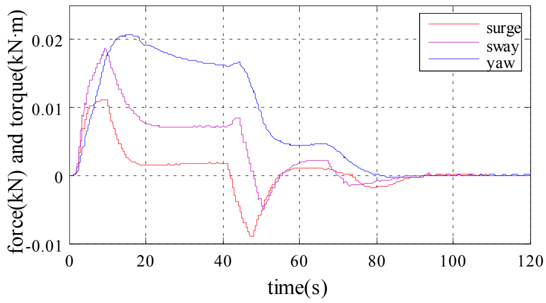

Fig. 13. The force and torque in calm water

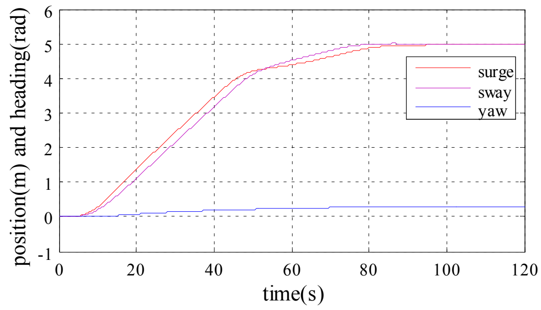

Fig. 14. The output curve in calm water

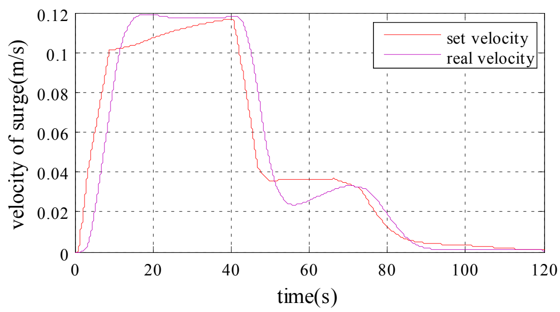

Fig. 15. Surge velocity in calm water

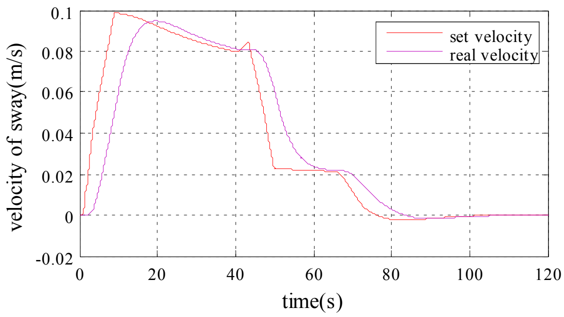

Fig. 16. Sway velocity in calm water

According to Figs. 13-14, force and torque change smoothly, which is easy to physical implementation. Displacement of Surge, sway and yaw angular process smoothly, and they have less overshoot. In Figs. 15-16, the process is divided into accelerating stage, constant high speed stage, decelerating stage, constant low speed stage and decelerating stage obviously.

In External Load Condition

In order to simulate external load, force disturbance and torque disturbance are added. The disturbance is within range of $1N(N\cdot m)-5N(N\cdot m)$. Initial set value is $(5m, 5m, 0.3rad)$. The simulation results in external disturbance condition are shown in Figures 17-20.

Compared with simulation in calm water, the amplitude of variation of control force and torque changed. The ship can continue to resist to the external load, and still keep position. The residual error is about $0.1m$ on surge direction and sway direction.

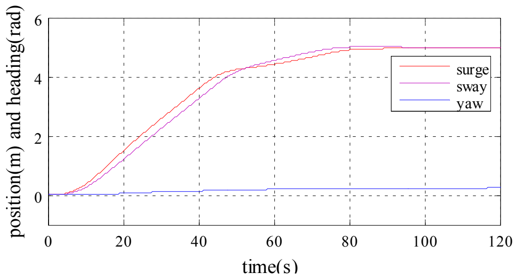

Fig. 17. Output curve in external load condition

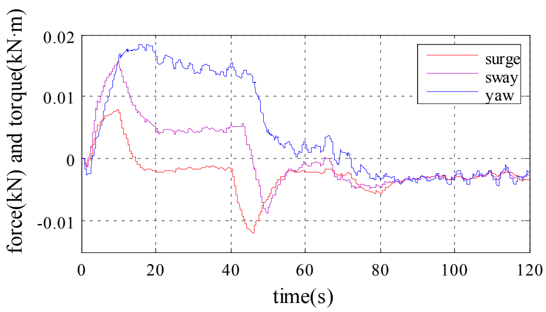

Fig. 18. Force and torque in external load condition

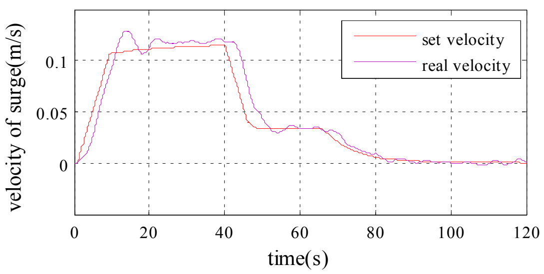

Fig. 19. Surge velocity in external load condition

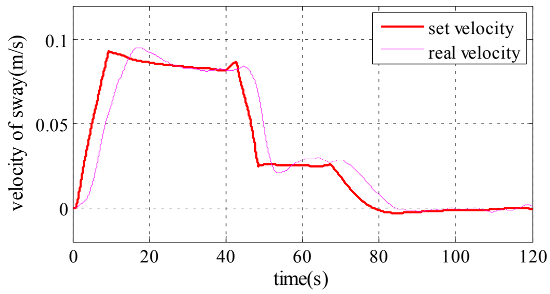

Fig. 20. Sway velocity in external load condition

Figs. 19-20 show the velocity accompany performance. Under the effect of external load, the velocity response follows the set curve, although the performance is less accuracy than that in calm water.

With Changed Model

As parameters of ship motion model are based on the numerical method, ship's accurate model is difficult to be determined. By adding object properties disturbance module, we simulate a changed controlled object. So the transfer function of the object will be dynamically changed. The simulation results are shown in Figures 21-22.

The response curves of controlled variable could slightly change. The result shows that the control method has good robustness. When the object is affected or the characteristics change, the decoupling matrix is not need to be redesigned, and the control performance basically keeps unchanged.

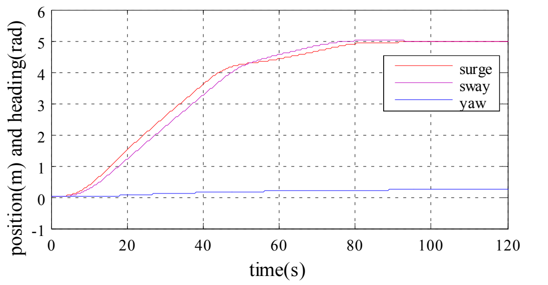

Fig. 21. Output curve with changed model

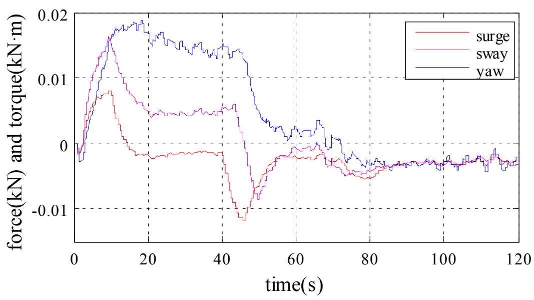

Fig. 22. Force and torque with changed mode

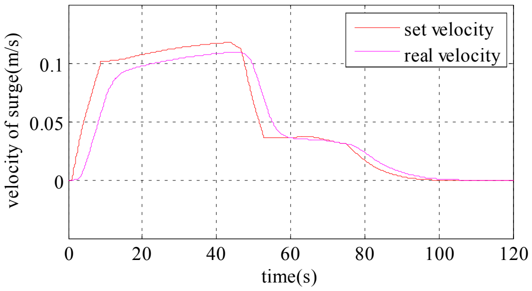

Fig. 23. Surge velocity with changed mode

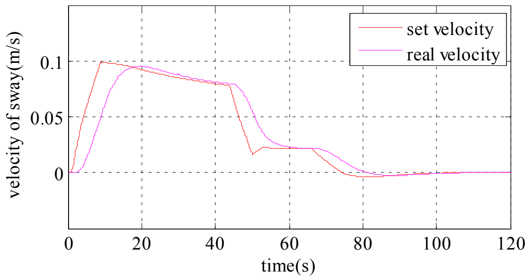

Fig. 24. Sway velocity with changed mode

Figures 23-24 show the velocity accompany performance. Comparatively, the effect on velocity response caused by uncertainness of model is less than that of external load.

In Fixed Point Positioning Mode

In fixed point positioning mode, set value is a point in fix coordinate system. In this mode, when ship is affected by environmental disturbance, and deviates from set position, ship can automatically move to its set position. The simulation results are shown in Figures 25-27.

(a)

(b)

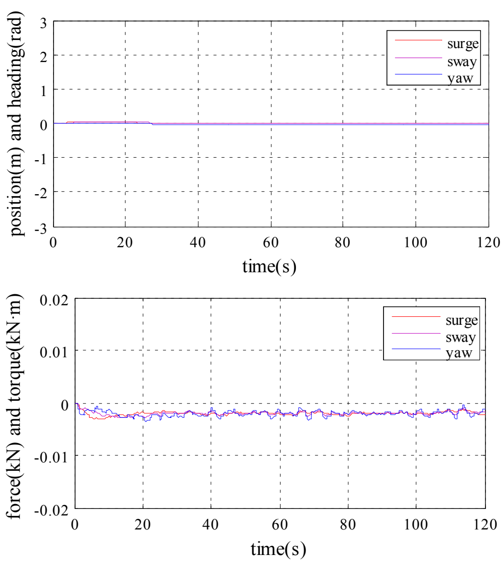

Fig. 25. In environmental disturbance of 1-3N: (a) position and heading; (b) force and torque

(a)

(b
)

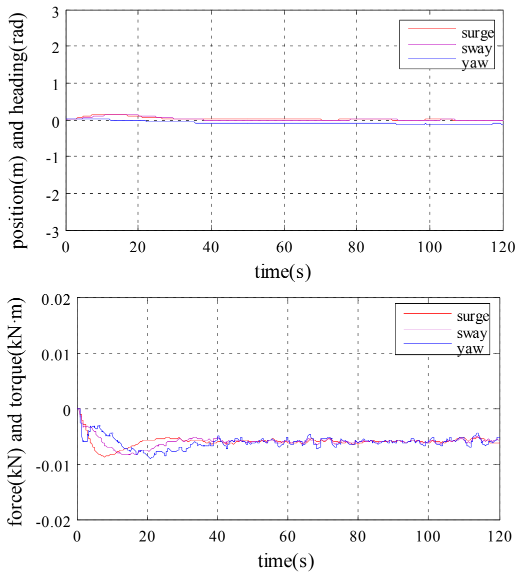

Fig. 26. In environmental disturbance of 5-7N: (a) position and heading; (b) force and torque

(a)

(b)

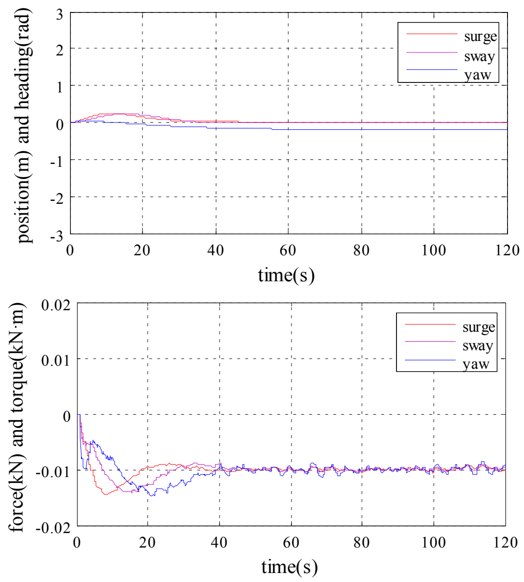

Fig. 27. Fixed point control mode in environmental disturbance of 9-11N: (a) position and heading; (b) force and torque

According to Figs. 25-27, if the environmental disturbance is under certain value (through more simulations, the largest disturbance value is $12N$), the designed control method satisfy fixed point control mode. At the beginning, external load will cause ship move away the set position, and then DPS gives force of opposing direction. The force can make ship return to its original position or near the position. The results show that larger external load will lead greater residual.

EXPERIMENTS

The aim of experiments carried out is to investigate and verify the proposed control algorithm applied to DPS. The experiments were carried out using the test ship, having a mass of $m = 0.754ton$, length of $L = 3.75m$ and breadth of $B = 0.86m$, as shown in Figure 28. The ship is equipped with three electric thrusters: two tunnel thrusters and two rudder thruster. The thrusters are located at the bottom of ship, as shown in Figure 29.

Fig. 28. Test ship

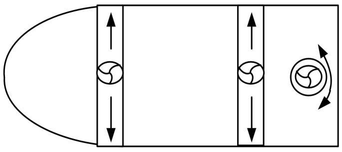

Fig. 29. Diagram of thruster allocation

The modules of these equipment and the proposed control method are entirely integrated into PC experimental platform. In order to compare the performance in different conditions, we conduct following five groups of experiments, as shown in Figures 30-34. Five groups of experiments show that in different condition, the proposed controller is able to force the ship to the desired position $(5m, 5m, 1rad)$ with high positioning accuracy as shown in table 2.

(a)

(b)

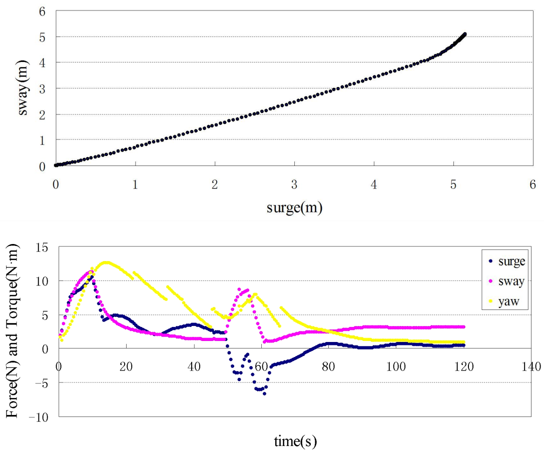

Fig. 30. Experiment in simulated wind class 1: (a) position; (b) force and torque

(a)

(b)

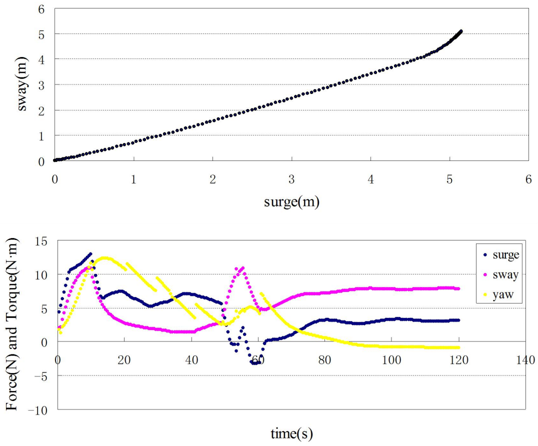

Fig. 31. Experiment in simulated wind class 3: (a) position; (b) force and torque

(a)

(b)

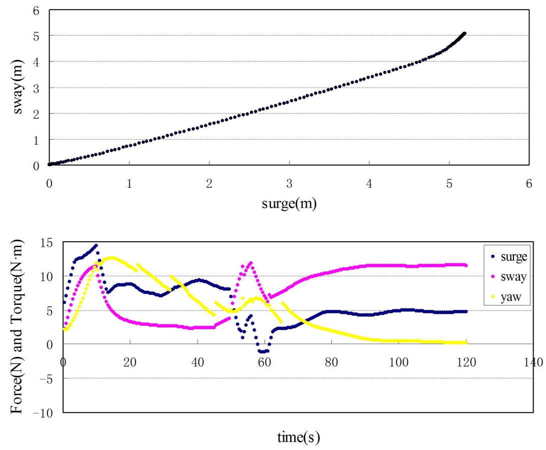

Fig. 32. Experiment in simulated wind class 5: (a) position; (b) force and torque

(a)

(b)

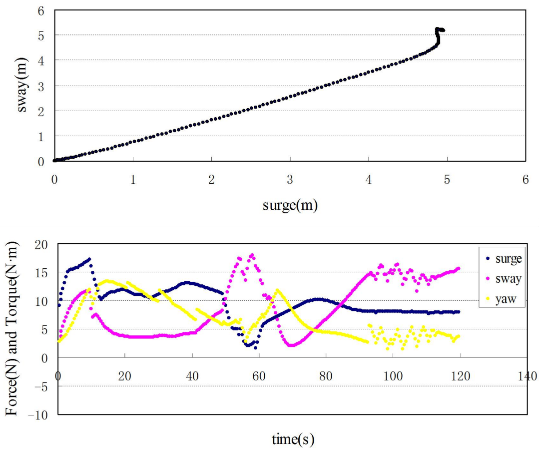

Fig. 33. Experiment in simulated wind class 8: (a) position; (b) force and torque

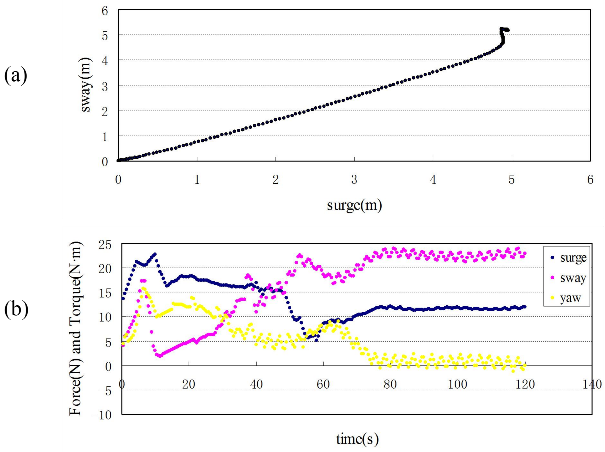

Fig. 34. Experiment in simulated wind class 10: (a) position; (b) force and torque

Table 2. Position accuracy

Condition	Wind Class 1	Wind Class 3	Wind Class 5	Wind Class 8
Positioning accuracy surge/sway	0.12m/ 0.09m	0.14m/ 0.08m	0.19m/ 0.07m	0.21m/ 0.11m

The results show quite a good overall agreement between the experimental and the simulation results. The curves of the surge control force, sway control force, and yaw control torque versus time are correspondingly shown. Under the wind condition of class 1 to class 5, the change of control force and control torque is smooth and reasonable.

Table 3 shows the success rate through thrust allocation algorithm. In the condition of wind class 1-10, control force and control torque can still satisfy allocation algorithm and guarantee a 100 percent success rate, which indicate that the outputs of designed controller are possible to be physically accomplished.

Table 3. Success rate of thrust allocation

Condition	Class 1	Class 2	Class 5	Class 8	Class 10
Succeed /100 Cycles	100	100	100	100	97

CONCLUSION

This paper proposed a dynamic positioning control law for DPS utilizing cascade control strategy. The outer loop controller based on subdivision control was designed to divide global state space into three subspaces. Aiming at respective subspace, specific motion mode was applied in order to make the control effect of whole positioning process achieve a relatively optimal state. The inner loop adopted hybrid fuzzy PID control based on fuzzy switching. Hybrid fuzzy PID controller guaranteed fast response and stable accuracy while fuzzy switching rules avoided the phenomenon of non-smooth switching process. Based on an input ship model, we considered changing environmental conditions and implemented a robust control design. Numerical simulations and experiments for the proposed control strategy were provided. Through simulations and experiments, whether external load increases or controlled object changes, positioning performance is nearly in accordance. Only when the environment become worse or the established mathematical model is not accurate at all, the change of force and torque is so severe that the thruster system can't work normally then the control system is not stable. Those results confirmed that subdivision control algorithm based on fuzzy-PID decoupling performed well when the ship was exposed to changes of environmental conditions, and it can effectively improve performance of the ship.

REFERENCES

Akasaka, N., "Design of piecewise linear LQ control by multivariable circle criterion for dynamic positioning system," The SICE-ICASE International Joint Conference, Busan (2006).

Bandyopadhyay, R. and Patranabis, D., "A new autotuning algorithm for PID controllers using dead-beat format," ISA Transactions, Vol. 40, pp: 255-266 (2001).

Boulkroune, A., Bounar, N., M'Saad, M. and Farza, M., "Indirect adaptive fuzzy control scheme based on observer for nonlinear systems: a novel SPR-filter approach," Neurocomputing, Vol. 135, pp: 378-387 (2014).

Bui, V-P., Ji, S-W., Choi, K-H. and Kim, Y-B., "Nonlinear observer and sliding mode control design for dynamic positioning of a surface ship," International Conference on Control, Automation and Systems, JeJu Island (2012).

Chang, W-J., Cheng, G-C. and Yeh, Y-L., "Fuzzy control of dynamic positioning systems for ships," Journal of Marine Science and Technology, Vol. 10, No.1, pp: 47-53(2002).

Chen, G., "Conventional and fuzzy PID controllers: an overview," International Journal of Intelligent Systems, Vol. 1, pp: 235-246 (1996).

Chen, X-T. and Tan, W-W., "An adaptive type-2 fuzzy logic controller for dynamic positioning," IEEE International Conference on Fuzzy Systems, Taipei (2011).

Dey, C. and Mudi, R-K., "An improved auto-tuning scheme for PID controllers," ISA Transactions, Vol. 48, No.4, pp: 396-409 (2009).

Ding, L. and Mao, X-G., "Dynamic positioning of ships using a planed neural network controller," Journal of Ship Research, Vol. 40, No. 2, pp: 164-171 (1998).

Dong, N-T., "Design of hybrid marine control systems for dynamic positioning," Ph.D. thesis, the National University of Singapore, Singapore (2006).

Fossen, T-I. and Grovlen, A., "Nonlinear output feedback control of dynamically positioned ships using vectorial observer backstepping," IEEE Trans. on Control Systems Technology, Vol. 6, No. 1, pp: 121-128 (1998).

Fossen, T-I., and Perez. T., "Kalman filtering for positioning and heading control of ships and offshore rigs," IEEE Control System, Vol. 29, No. 6, pp: 32-46 (2009).

Grorvlen, A. and Fossen, T-I., "Nonlinear control of dynamic positioned ships using only position feedback: an observer backstepping approach," Proceedings of the 35th Conference on Decision and Control, Kobe (1996).

Jia, B-Z., Ren, G. and Xiu, Z-H., "Fuzzy switching controller for multiple model," The 2nd International Conference on Fuzzy Systems and Knowledge Discovery, Changsha (2005).

John. F., Michael, J-G. and Basil, K., "A comparison of characteristic locus and optimal designs for dynamic ship positioning systems," IEEE Transactions on Automatic Control, Vol. 27, No. 6, pp: 1143-1157 (1982).

Kim, J-H. and Oh, S-J., "A fuzzy PID controller for non-linear and uncertain systems," Soft Computing, Vol. 4, No. 2, pp: 123-129 (2000).

Kim, M.H., "Nonlinear control and robust observer design for marine vehicles," Ph.D. thesis, Virginia Polytechnic Institute and State University, Virginia, USA (2000).

Liu, F-R., Chen, H. and Gao, H-B., "Application of moving horizon filter for dynamic positioning ship," Journal of Wuhan University of Technology, Vol. 32, No. 12, pp: 117-120 (2010).

Liu, R., Wang, X-Y. and Huang, X-C., "Hybrid fuzzy PID control of hydraulic robot," ASME International Mechanical Engineering Congress and Exposition, New Orleans (2002).

Li, W., "Design of a hybrid fuzzy logic proportional plus conventional integral-derivative controller," IEEE Transactions on Fuzzy Systems, Vol. 6, No. 4, pp: 449-463 (1998).

McGookin, E-W., Murray-Smith, D-J., Li, Y. and Fossen, T-I., "Ship steering control system optimisation using genetic algorithms," Control Engineering Practice, Vol. 8, No. 4, pp: 429-443 (2000).

Parnichkun, M. and Ngaecharoenkul, C., "Kinematics control of a pneumatic system by hybrid fuzzy PID," Mechatronics, Vol. 11, No. 8, pp: 1001-1023 (2001).

Tee, K-P. and Sam, S-Z., "Control of fully actuated ocean surface ships using a class of feedforward approximators," IEEE Transactions on Control Systems Technology, Vol. 14, No. 4, pp: 750-756 (2006).

Verma, R-K., "Dynamic positioning of ship using direct model reference adaptive control," M.S. thesis, College of Graduate Studies Texas A&M University-Kingsville, Texas, USA (2004).

Wang, L-Y., Xiao, J-M. and Wang, X-H., "Ship dynamic positioning systems based on fuzzy predictive control," Telkomnika, Vol. 11, No. 11, pp: 6769-6779 (2013).

Wang, Y., and Jia, B-Z., "Fuzzy switching PID controller for ship motion," Navigation of China, Vol. 4, pp: 30-34 (2006).

Zhang, C-D., Wang, X-H. and Xiao, J-M., "Ship dynamic positioning system based on backstepping control," Journal of Theoretical and Applied Information Technology, Vol. 51, No. 1, pp: 129-136 (2013).

基於分段模糊PID解耦的船舶動力定位控制演算法

黎洪生　　王猛　　苗青
武漢理工大學機電工程學院

Thierno-Mamadou-Pathe Diallo
Faculty of Science,
Centre Universitaire de Kindia

摘 要

動力定位是指船舶依靠自身的動力在海洋中保持一定的位置，由於船舶運動的複雜性和海洋環境的不確定性，導致船舶動力定位是一個複雜的系統。本文提出了一種基於分段模糊PID解耦的船舶動力定位控制演算法，並將其應用於在外力作用下的船舶位置控制。根據船舶運動模型，在內環採用解耦控制方法消除變數之間的耦合。採用模糊-PID雙模控制用於控制速度和角速度。採用模糊切換邏輯(FSL)來減小模糊PID雙模控制器的切換干擾。外環採用分段控制策略控制位置和航向。該方法構成了串級控制系統，用於實現精確的定位。通過模擬和實驗驗證了該控制方法具有定位精度高、對環境適應性強、魯棒性強等優點。